2014

Innovative Minichannel Condensers and Evaporators for Air Conditioning Equipment

Davide Del Col
University of Padova, Italy, davide.delcol@unipd.it

Marco Rossato
University of Padova, Italy, marco.rossato.1@unipd.it

Stefano Bernardinello
Blue Box – Swegon, Italy, Stefano.Bernardinello@Swegon.it

Luca Zaramella
University of Padova, Italy, luzara@hotmail.it

Innovative Minichannel Condensers and Evaporators for Air Conditioning Equipment

Davide DEL COL[1,*], Marco ROSSATO[1], Stefano BERNARDINELLO[2], Luca ZARAMELLA[1]

[1] Department of Industrial Engineering, University of Padova
Via Venezia 1 – 35131 Padova, Italy

[2] Blue Box Group S.r.l. – Swegon Group
Via Valletta, 5 - 30010 Cantarana di Cona (VE), Italy

* Corresponding Author
Tel.: +39 049 8276891; Fax: +39 049 8276896; Email: davide.delcol@unipd.it

ABSTRACT

The use of aluminum heat exchangers for refrigeration and air-conditioning equipment is very interesting since it allows to reduce weight and manufacturing costs while maintaining high performance. In this paper a two-phase heat transfer characterization of an innovative aluminum minichannel heat exchanger is presented.
The heat exchanger is composed by rectangular channels with internal perforated turbulators. A unique test section has been designed and realized in the Two Phase Heat Transfer Lab of the University of Padova in order to measure the refrigerant heat transfer coefficient (HTC) during flow boiling and condensation. The test section has a single refrigerant channel with a perforated fin to make the minichannels. The test section is provided with 14 water flow modules installed at top and bottom of the refrigerant channel to promote boiling or condensation of the refrigerant. Therefore, the test section is divided in seven different zones: each of them is equipped with 8 thermocouples to measure the wall temperature during the refrigerant phase change. The heat flow rate in each zone is calculated from an energy balance on the water side. Pressure transducers and thermocouples on the refrigerant side allow to determine the saturation temperature and thus the heat transfer coefficient of the refrigerant. The refrigerant used during tests is R410A.
The particular scheme adopted for the test section enables to measure HTC at varying vapor quality and heat flow rate. Vaporization and condensation tests were carried out with different saturation temperatures, heat flux (from 10 to 60 kW m^{-2}) and refrigerant mass flux (50–100 kg $s^{-1}m^{-2}$).
The aim of the present paper is to investigate the potential performance of these innovative minichannel heat exchangers as condensers and evaporators in air-conditioning equipment, since very few data are available in the literature during flow boiling and condensation in similar geometries. Therefore, it is very important to verify the accuracy of available heat transfer predicting models. The present preliminary flow boiling data have been compared with predictions from the Liu and Winterton (1991) correlation.

1. INTRODUCTION AND LITERATURE REVIEW

Compact aluminum heat exchangers are used in various applications such as electronic cooling devices, cryogenic heat exchangers, automobile radiators, but their application in the field of air conditioning is still limited and little studied.
The use of aluminum minichannels heat exchangers with high ratio of exchange surface area / volume for air conditioning application allows to obtain high performance of heat exchange with a limited refrigerant charge.
Highly efficient heat transfer is critical to develop technologies with less environmental impact. In this case, an efficient and compact solution allows a reduction of greenhouse gas emissions resulting from electricity consumption and allows a reduction of the refrigerant charge resulting in lower potential emissions of refrigerants.
They are available in a wide variety of geometries: turbulator with offset strip fins (Fig. 1) and turbulator with perforated fins (Fig. 4) are the most used.
In the literature, there are numerous studies on heat transfer in single-phase flow for aluminum compact heat exchangers. Kays (1972) presented an analytical model of the heat transfer and friction factor losses in offset strip

fin surfaces. This is one of the first attempts to propose a model that includes the form drag contribution of the blunt fin edges.
Wieting (1975) evaluated the effect of fin length, height, thickness, spacing and hydraulic diameter on the performance and developed empirical relationships correlating experimental heat transfer and flow friction data for rectangular offset plate fin heat exchangers configurations given by London and Shah (1968), Walters (1969) and Kays and London (1964) for laminar or turbulent flow.
These correlations can be applicable only for air or gas as the heat transfer fluid and should be used only in completely turbulent or laminar regime.
Manglick and Bergles (1995) reanalyzed the data reported in the literature for the rectangular offset strip fin compact heat exchangers and presented a generalized correlation for f (friction factor) and j (Colburn factor) that fit the experimental data for different airflows. Their correlations may be applicable for all gases and most liquids with moderate Prandtl number (fluids with Prandtl numbers ranging from 0.5 to 15) because the experimental data were obtained using air (Pr = 0.7) in the $120 < Re < 10^4$ range. Their equations represent the data continuously in the laminar, transition, and turbulent flow regions.
Min-Soo Kim et al. (2011) investigated the thermo-flow characteristics of a heat exchanger with offset strip fins for various fin geometries and working fluids. They observed that previous correlations underestimate *f* values in the laminar and turbulent regimes and overestimate *j* values in the laminar regime, as the blockage ratio increases. Therefore, they presented a new correlation for blockage ratios greater than 20%. While most previous correlations was limited to air, the study by Min-Soo Kim considered various working fluids, but all related to single phase heat transfer. Moreover, new *j* equations were suggested as functions of the Prandtl number to correlate the experimental values for various working fluids. Therefore, the correlations proposed could be available for a wide ranges of blockage ratios (0–35%) and Prandtl numbers (0.72–50).

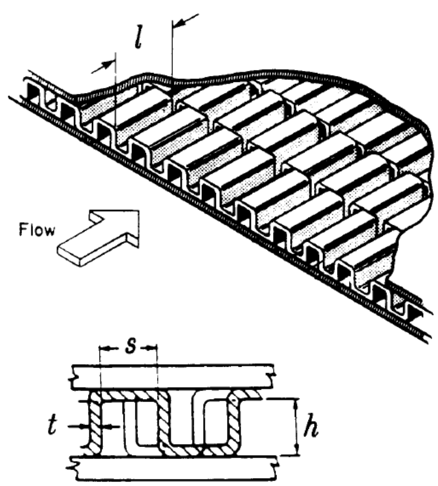

Figure 1. Offset strip fin turbulator (Manglick and Bergles (1995)).

Differently from the case of sensible heating and cooling, very limited studies are available with phase change in such geometries. With reference to two-phase flow, Mandrusiak and Carey (1989) investigated different offset strip fins geometries, while Robertson and Clarke (1985) studied perforated fins with liquid nitrogen.
Feldman et al. (1999) studied the heat flow rate in flow boiling for heat exchangers with vertical channels 'offset strip fins' and 'perforated fins' for the refrigerant CFC114. The vaporization of the fluid was obtained with foil resistances placed above and below the channel of the refrigerant. It was investigated a wide range of quality, specific mass flow rates up to 45 kg $s^{-1}m^{-2}$, heat flow rates equal to 3.5 kW m^{-2} and pressures up to 3 bar.
However, only few studies are reported in the literature regarding the performance in phase change heat transfer of these heat exchangers and their application in refrigeration and air conditioning equipment needs more extended investigation.
In order to investigate the heat transfer coefficients in the two-phase flow with heat fluxes up to 60 kW m^{-2} a new test section is here presented.
The test section has been designed with a refrigerant channel with perforated turbulator that exchanges heat with water flowing above and below in cross flow in channels with offset strip fins turbulator.

In the present study, the heat transfer during vaporization and condensation with refrigerant R410A is studied. During the tests, the heat flow rate is governed by controlling the inlet water temperatures.
In the design of the test section particular attention has been paid to the wall temperature measurement in order to determine the heat transfer coefficient of the refrigerant with high accuracy.

2. EXPERIMENTAL APPARATUS

The experimental tests have been performed at the Two-Phase Heat Transfer Laboratory of the Dipartimento di Ingegneria Industriale of the University of Padova. Figure 2 shows a scheme of the facility used. A Coriolis effect mass flow meter measures the refrigerant mass flow rate (accuracy of ±0.2% of the measured value) while it passes through the circuit driven by a magnetically coupled gear pump. The inner pressure of the system can be varied by means of a bladder accumulator. During condensation tests the refrigerant flows through two tube-in-tube heat exchangers to reach superheated vapor conditions before the test section, while in vaporization tests a by-pass allows the refrigerant to reach the test section still as subcooled liquid. Before the test section some water flowing in countercurrent and coming from a thermostatic bath is used to induce the refrigerant to reach the desired conditions, i. e. 5 K of superheating during condensation tests or subcooling during flow boiling tests, in order to avoid phase change outside the test section and possible maldistribution. After the test section the refrigerant is subcooled in a brazed plate heat exchanger by a chiller that operates with brine. The experimental tests shown in this paper have been obtained during vaporization at saturation temperature ranging between 17 and 20 °C and during condensation at saturation temperature of 40 °C.

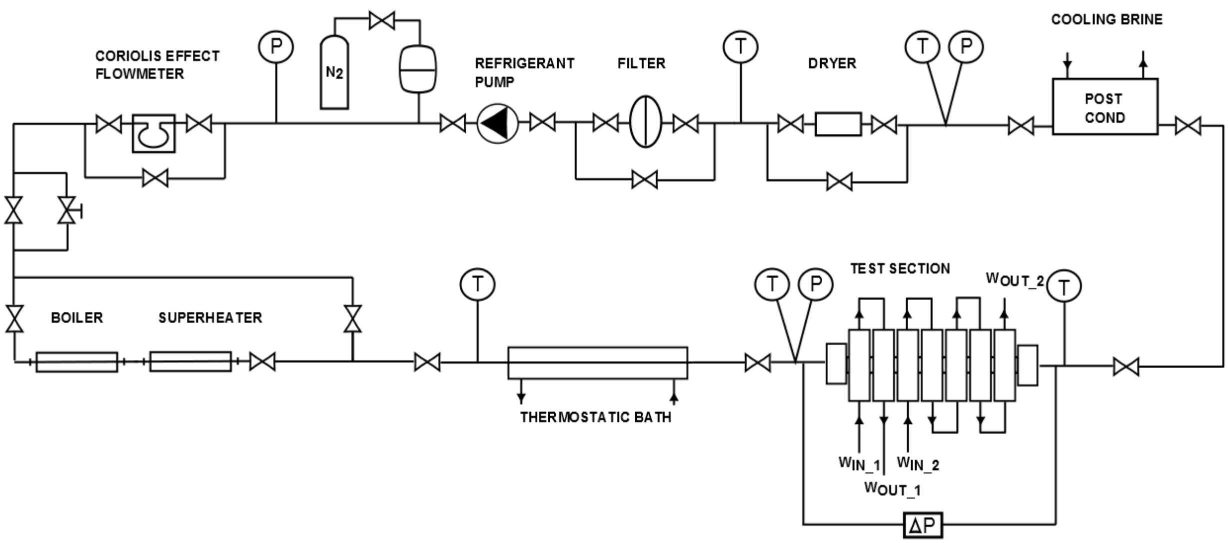

Figure 2. Schematic of the experimental test apparatus.

2.1 Test section for heat transfer coefficients measurements

The test section (shown in Figure 3) is composed of a single refrigerant channel, 0.5 m long, with perforated fins inside (as represented in Figure 4), and 14 water modules bonded on the external surfaces, using an aluminum based conductive paste. The refrigerant channel is 58 mm wide and 3 mm high, filled with perforated fins: the hydraulic diameter is equal to 1.8 mm while the passage area is equal to 127 mm^2, considering and obstruction of 27 %. Two grooves have been made on the refrigerant wall for each water module so that 4 thermocouples (0.4 mm in diameter) have been placed before bonding the water modules to the refrigerant channel. The position of the thermocouples is represented with red dots in Figure 5. Therefore, the refrigerant wall temperature is measured by means of 56 T-type thermocouples. These thermocouples were calibrated using a superthermometer with a thermistor standard probe

(0.001 K accuracy) and the zero for the cold junction is made using a Kaye reference device. The accuracy of thermocouples is ± 0.05 K.

Figure 3. Picture of the test section before insulation.

Each of the 7 subsections of the refrigerant channel exchanges heat with water in cross flow. The two water modules attached to the same refrigerant subsection are connected in parallel (as shown in Figure 5), while the connections between different water modules are represented in Figure 2. The resulting configuration for refrigerant and water is a nearly co-current flow. For each couple of water modules a calibrated T-type thermopile (accuracy ±0.03 K) measures the water temperature change.
Two thermocouples, an absolute pressure transducer (reported accuracy of 0.025% of the full scale) and a differential pressure transducer measure the refrigerant conditions at the entrance and exit of the test section.

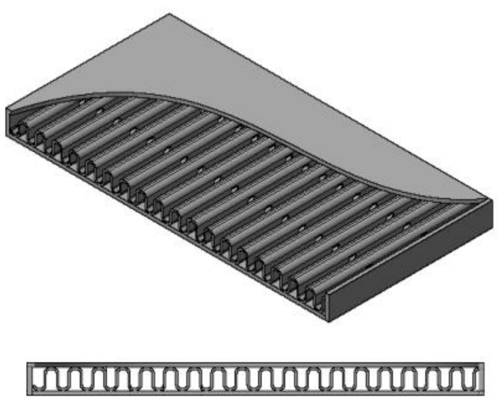

Figure 4. Perforated fins inside the refrigerant channel.

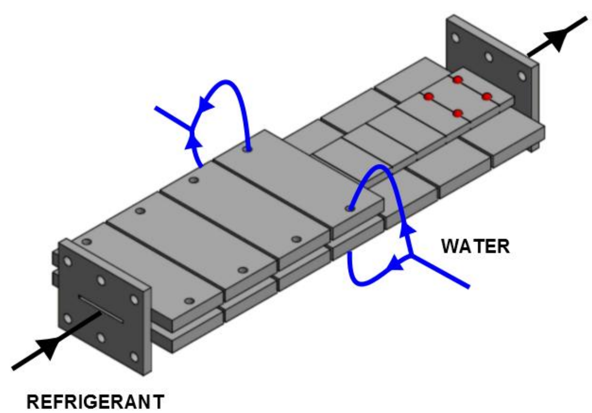

Figure 5. Test section with water modules: the last three water modules are not depicted. The position of the thermocouples, for a single water module, is represented with red dots.

3. DATA REDUCTION

The heat flow rate exchanged by every refrigerant subsection (Q_{subsec}) is calculated from a thermal balance on the water side as:

$$Q_{sub\sec} = \dot{m}_w c_{pw} \left|\Delta T_w\right| \tag{1}$$

The heat transfer coefficient is then calculated for every subsection as

$$HTC = \frac{Q_{sub\sec}}{A_{sub\sec}\Delta T_{wall\_sat}} = \frac{q}{\Delta T_{wall\_sat}} \tag{2}$$

where q is the heat flux in the subsection, and ΔT_{wall_sat} is the temperature difference between the wall temperature and the refrigerant saturation temperature. A_{subsec} does not consider the perforated fins and is composed by the two rectangular areas that divide the refrigerant from water above and below.
During condensation tests $\Delta T_{wall\_sat} = T_{sat} - T_{wall}$, while in vaporization tests $\Delta T_{wall\_sat} = T_{wall} - T_{sat}$.
The wall temperature is calculated as the mean value of the 8 thermocouples positioned in the subsection, each one is corrected to account for the temperature variation across the aluminum wall ΔT_{wall} as reported in Eq. 3, where λ_{al} is the aluminum thermal conductivity and s_{wall} is the aluminum thickness.

$$\Delta T_{wall} = \frac{q}{\lambda_{al}} s_{wall} \tag{3}$$

The enthalpy of the refrigerant at the inlet of the test section results from the measured values of temperature and pressure of the superheated vapor, during condensation tests, or of the subcooled liquid, during flow boiling test runs. Since the heat exchanged by the refrigerant in the subsection is equal to that exchanged by water, it is possible to get the enthalpy and the vapor title at the exit of each subsection. Eq. 4 is reported for vaporization but it can be easily modified for condensation.

$$h_{out} = \frac{Q_{sub\sec}}{\dot{m}_r} + h_{in} \tag{4}$$

$$x_{out} = \frac{h_{out} - h_l}{h_{lv}} \tag{5}$$

The experimental uncertainty analysis has been done in agreement with the guidelines provided by ISO (1995).
The standard uncertainty is obtained by combining type A (u_A) and type B (u_B) uncertainties:

$$u = \sqrt{u_A^2 + u_B^2} \tag{6}$$

In order to get the standard uncertainty of indirect measurements the law of uncertainty propagation is used. For example, starting from Eq. (1) and Eq. (2), the standard uncertainty of the heat transfer coefficient is

$$u_{HTC} = \sqrt{\left(\frac{c_{p,w}\Delta T_w}{A_{sub\sec}\Delta T_{wall\_sat}} u_{\dot{m}_w}\right)^2 + \left(\frac{c_{p,w}\dot{m}_w}{A_{sub\sec}\Delta T_{wall\_sat}} u_{\Delta T_w}\right)^2 + \left(\frac{HTC}{\Delta T_{wall\_sat}} u_{(\Delta T_{wall\_sat})}\right)^2} \tag{7}$$

The uncertainty in measured HTC is around 10% when q = 20 kW m^{-2}, while it is lower than 10% for q > 20 kW m^{-2} and becomes lower than 5% for q > 30 kW m^{-2}.

4. EXPERIMENTAL RESULTS

Table 1 reports the operating conditions during the test runs. During each test run seven operating conditions are tested, one for each subsection and therefore seven values of the heat transfer coefficient are measured, one for each experimental module.
The test runs have been performed at G_r = 50–100 kg m^{-2} s^{-1} during condensation and G_r = 50 kg m^{-2} s^{-1} during flow boiling where $G_r = \dot{m} / A_c$ with A_c area of the channel perpendicular to the refrigerant flow, considering the turbulator obstruction.

Table 1. Operating test conditions and number of data points.

Parameter	**Mean Value / Range**	
	Condensation	Vaporization
Dew / bubble temperature [°C]	40	17–20
Saturation pressure [bar]	24.3	13.3–14.5
Vapor quality [-]	0–1	0–0.7
Refrigerant mass velocity [kg m^{-2} s^{-1}]	50–100	50
Heat flux [kW m^{-2}]	10–60	10–60
Superheating / Subcooling at inlet [K]	5	5

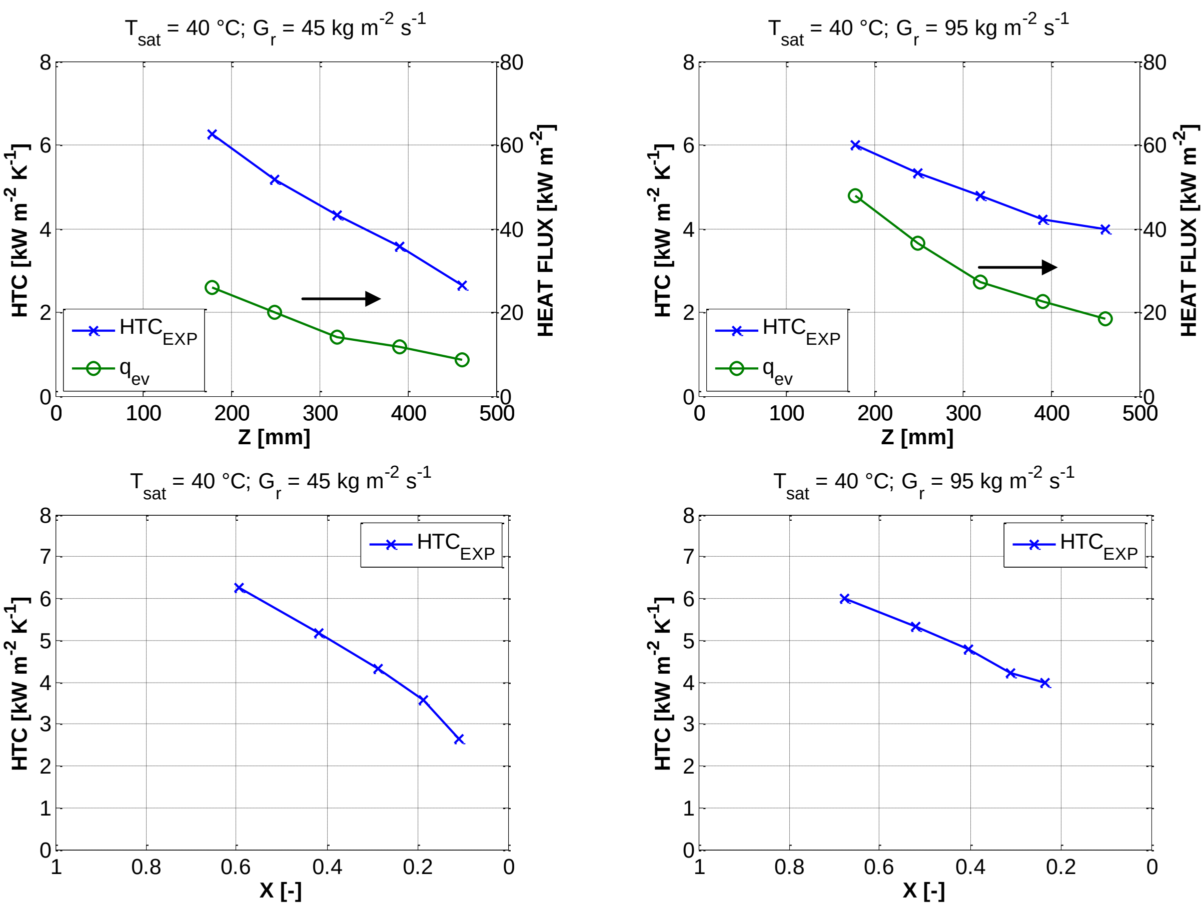

Figure 6. Heat transfer coefficients versus axial position (up) and versus vapor quality (below) during a single condensation test with G_r = 45 kg m^{-2} s^{-1} (left) and G_r = 95 kg m^{-2} s^{-1} (right). T_{sat} = 40 °C. ΔT_{wall_sat} varies between 3 and 7 K. The upper graph reports the heat flux for each subsection.

4.1 Condensation tests

Test runs have been performed at 40 °C. Some results are reported in Figure 6. The two upper graphs of Fig. 6 show the heat transfer coefficients measured along the test section during two test runs with refrigerant mass velocity of 45 and 95 kg m^{-2} s^{-1} respectively. The heat flux during the test runs is also depicted. The bottom graphs of Fig. 6 show the heat transfer coefficients versus the mean vapor quality for the same two test runs.
Fig. 7 reports the heat transfer coefficient (HTC) versus vapor quality for tests with refrigerant mass velocity equal to 50 and 100 kg m^{-2} s^{-1}.
The experimental trends in Figures 6 and 7 show that the heat transfer coefficient decreases as the condensation proceeds and vapor quality diminishes, as one would expect. By comparing the test results in Fig. 6 and Fig. 7, it seems that the heat transfer coefficients are higher at the lower mass flux but it is important to note that the heat flux varies, and therefore the temperature difference between saturation and wall changes, too. From the data it can be seen that the heat transfer coefficient is roughly the same for the two values of mass flux at the same quality, and the scattering is mainly due to the variation in temperature difference (saturation minus wall): as expected, at the same vapor quality, higher heat transfer coefficient corresponds to lower temperature difference.

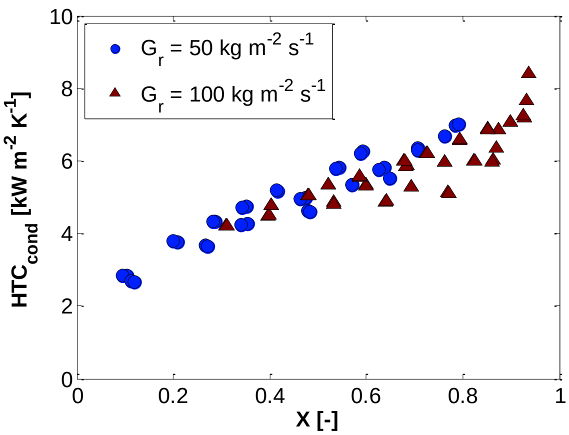

Figure 7. Heat transfer coefficient versus vapor quality during condensation tests with refrigerant mass velocity of 50 and 100 kg s^{-1} m^{-2}. Saturation temperature is equal to 40°C.

4.2 Vaporization tests

Flow boiling tests are performed at saturation temperature ranging between 17 and 20 °C. Some preliminary data are reported in Figs 8 and 9. Figure 8 shows the trend of the refrigerant heat transfer coefficient along the test section for one test run. The first two subsections are used to get the subcooled liquid to the saturated conditions, thus the corresponding values are not reported. Figure 9 shows the heat transfer coefficient (HTC) versus vapor quality for the same test run. Both graphs report the heat flux for each module.
From Figs. 8 and 9, it can be seen that the heat flux is not constant along the channel, but it diminishes as the vaporization proceeds and vapor quality increases. In the present test runs, the heat transfer coefficient decreases too. One possible reason for the decrease of the heat transfer coefficient at high values of vapor quality may be the partial dry-out of the liquid film. Unfortunately, since the heat flux is a dependent variable, it is not easy to separate the effect of heat flux from the effect of vapor quality, and therefore much more data are needed to compare the experimental trends of the present heat transfer coefficients to those measured with Joule effect heating, at constant heat flux.
Because no predicting model has been developed for similar geometries, some comparison of the present preliminary data can be done with flow boiling models available in the open literature for conventional channels. Therefore, in the following, the heat transfer coefficients measured during vaporization tests have been compared with the predictions obtained from the Liu and Winterton (1991) correlation. This correlation, shown in Eq. 8, combines the Dittus Boelter equation for forced liquid convection (Eq.9), multiplied by an enhancement factor *F*

(Eq.11), with the Cooper correlation (Eq.10) for pool boiling inside tubes (thus the constant 55 is changed to 85), multiplied by a suppression factor *S* (Eq 11).

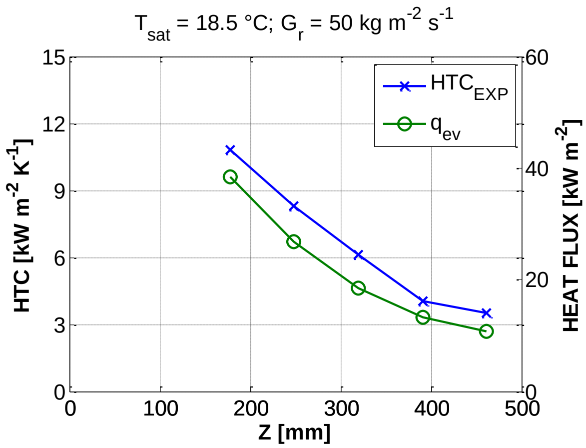

Figure 8. Heat transfer coefficients and heat flux measured along the test section during a single vaporization test with G_r = 50 kg s^{-1} m^{-2} and T_{sat} = 18.5 °C.

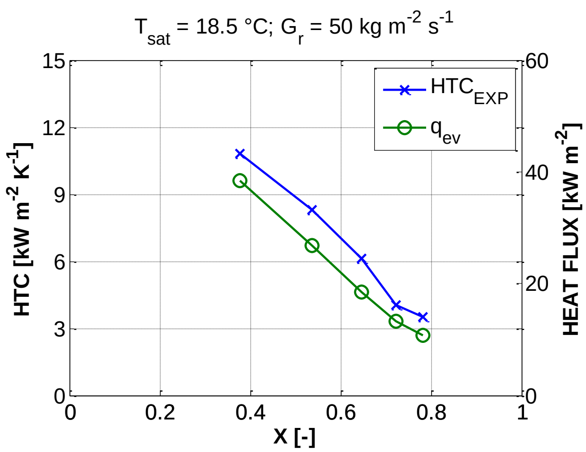

Figure 9. Heat transfer coefficients and heat flux versus vapor quality during a single vaporization test with G_r = 50 kg s^{-1} m^{-2} and T_{sat} = 18.5 °C.

In order to compare the experimental data with the correlation by Liu and Winterton (1991), the heat flux and the heat transfer coefficient are hereafter referred to the total heat transfer area, including the perforated fins, assuming an efficiency of the fins equal to one. The diameter is the hydraulic diameter of the channels created by the turbulators.

$$HTC_{LW} = \left(\left(F\ HTC_F \right)^2 + \left(S\ HTC_{PB} \right)^2 \right)^{0.5} \tag{8}$$

$$HTC_F = 0.023 \left(\frac{\lambda}{d_h} \right) \mathrm{Re}_l^{0.8}\, \mathrm{Pr}_l^{0.4} \tag{9}$$

$$HTC_{PB} = 85 P_{red}^{0.12}\, \mathrm{q}^{(2/3)} \log_{10}\left(P_{red}^{-0.55} \right) M^{-0.5} \tag{10}$$

$$F = \left(1 + X\,\mathrm{Pr}_l \left(\frac{\rho_l}{\rho_v - 1}\right)\right)^{0.35} \qquad S = \left(1 + 0.055\,F^{0.1}\,\mathrm{Re}_l^{\,0.16}\right)^{-1} \tag{11}$$

Figure 10 compares the experimental heat transfer coefficients with those calculated using the Liu and Winterton (1991) correlation at the same operating conditions. Since a complete analysis of the dry-out conditions in these channels has not been performed yet, the heat transfer coefficients used for the comparison are limited to the maximum value of 0.6 vapor quality.
As it can be seen in Fig. 10, the present model is not able to predict the present experimental data with sufficient accuracy; besides, the deviations between calculated and measured values display high scattering and this would mean that the model is not able to catch the experimental trends. However, a more extensive experimental campaign is needed to assess the available predicting models.

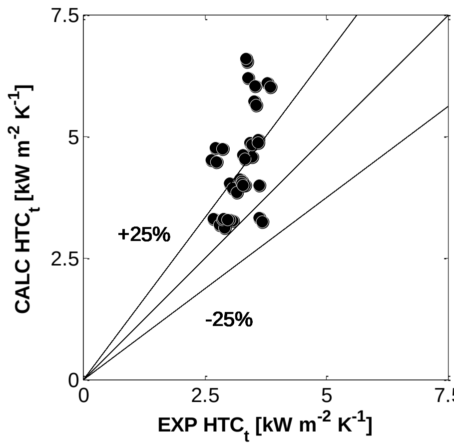

Figure 10. Heat transfer coefficients calculated with Liu and Winterton (1991) correlation versus experimental values for vapor quality between 0.2 and 0.6. The refrigerant mass velocity is equal to 50 kg $m^{-2}s^{-1}$, the saturation temperature is equal to 18 °C.

7. CONCLUSIONS

A new test section has been developed and described in this paper. This new facility allows to test minichannel heat exchangers with turbulators inside, both during condensation and flow boiling. In this paper an innovative aluminum heat exchanger has been tested with R410A and the local heat transfer coefficients have been measured during vaporization and condensation. This kind of geometry has been tested by other authors in single phase flow but very limited results are available on two phase heat transfer and therefore the present study can be very important for refrigeration and air conditioning applications. Further investigations will be accomplished in order to better understand the behavior of this geometry and its potential performance in air conditioning applications.

NOMENCLATURE

A	surface area (m^2)	*d*	diameter (m)
F	enhancement factor (-)	*G*	mass velocity (kg m^{-2} s^{-1})
HTC	heat transfer coefficient (W m^{-2} K^{-1})	*h*	specific enthalpy (J kg^{-1})
M	molecular weight	$\dot{m}$	mass flow rate (kg s^{-1})
p	pressure (Pa)	Pr	Prandtl number (-)
q	heat flux (W m^{-2})	*Q*	heat flow rate (W)
S	suppression factor (-)	*T*	temperature (°C)

Re	Reynolds number (-)	*z*	axial position (m)
x	thermodynamic vapor quality (-)		

Greek symbols

ΔT	temperature difference (K)	ρ	density (kg m^{-3})
λ	thermal conductivity (W $m^{-1}K^{-1}$)	σ_N	standard deviation (%)

Subscripts

al	aluminum	*c*	channel
EXP	experimental	*h*	hydraulic
l	liquid	*LW*	Liu and Winterton
PB	pool boiling	*red*	reduced
sat	saturation condition	*subsec*	referred to a single subsection
r	refrigerant	*t*	referred to the total heat transfer area
v	vapor	*w*	water
wall	referred to aluminum wall		

REFERENCES

ISO, *Guide to the Expression of Uncertainty in Measurement*, 1995.

Kays, W. M., *Compact Heat Exchangers*, AGARD Lecture Ser. No. 57 on Heat Exchangers, AGARD-LS-57-72, NATO, Paris, 1972.

Kays, W. M., and London, A. L., *Compact Heat Exchangers*, 2nd ed., McGraw-Hill, New York, 1964.

Lemmon, E.W., Huber, M.L., McLinden, M.O., *NIST Standard Reference Database 23: Reference Fluid Thermodynamic and Transport Properties-REFPROP, Version 9.1*, National Institute of Standards and Technology, Standard Reference Data Program, Gaithersburg, 2013.

Liu Z., Winterton R. H. S., A general correlation for saturated and subcooled flow boiling in tubes and annuli based on a nucleate pool boiling equation, Int. J. Heat and Mass Transfer, 34, 2759-2766, 1991.

London, A. L., and Shah R. K., *Rectangular Plate-Fin Surfaces—HeatTransfer and Flow Friction Characteristics,*Trans. ASME, J. Eng. Power 90, 218-228, 1968.

Mandrusiak G. D., Carey V. P., *Convective boiling in vertical channels with different offset strip fin geometries,* Journal of Heat Transfer, v. 111, n. 1, pp. 156-165, Feb. 1989.

Manglik Ray M., Bergles A. E., *Heat Transfer and Pressure Drop Correlations for the Rectangular Offset Strip Fin Compact Heat Exchanger*, Experimental Thermal and Fluid Science, 10:171-180, 1995.

Min-Soo Kim et al., *Correlations and optimization of a heat exchanger with offset-strip fins;* International Journal of Heat and Mass Transfer, v 54, n 9-10, p 2073-9, April 2011.

Robertson J. M., Clarke R. H., *General prediction of convective boiling coefficients in plate-fin heat exchanger passages*, 23rd National Heat Transfer Conference, Denver; AIChE Symposium Series, n. 245, pp. 129-134, 1985.

Wieting, A. R., *Empirical Correlations for Heat Transfer and Flow Friction Characteristics of Rectangular Offset-Fin Plate- Fin Heat Exchangers,* Trans. ASME, J. Heat Transfer 97, 488-490, 1975.